Erosional narrowing after dam removal: Theory and numerical model

M. Wong[1,2], A. Cantelli[1,3], C. Paola[1,4] and G. Parker[1,5]

[1]National Center for Earth-surface Dynamics, St. Anthony Falls Laboratory, Department of Civil Engineering, University of Minnesota, #2 3rd Ave SE, Minneapolis, MN 55414; PH (612)624-4675; FAX (612)624-4363; email: [2]wong0228@umn.edu; [3]cante004@umn.edu; [4]cpaola@umn.edu; [5]parke002@umn.edu

Abstract (#4144)

Experiments carried out in a flume at St. Anthony Falls Laboratory, University of Minnesota have shown an interesting phenomenon herein called "erosional narrowing". This occurs immediately after the sudden removal of a dam that is filled with sediment. A channel incises into the deposit after failure of the leading front of the sediment deposit. In the early stages of incision this channel may become significantly narrower as it undergoes degradation. Both incision and narrowing propagate upstream in a relatively short time. In the long term however, the depositional contribution from the side slopes eventually balances and then surpasses erosional narrowing, so the channel widens toward some new equilibrium state with a lower streamwise slope. This picture is at variance with the general belief that the incisional channel widens from the very beginning. A simplified 1-D model of the phenomenon is developed and implemented numerically; in it the time evolution of channel width depends on the streamwise gradient of sediment transport and fluvial erosion of the channel banks (sidewalls).

Introduction

One of the ten recommendations given by the ASCE Task Committee on Hydraulics, Bank Mechanics, and Modeling of River Width Adjustment (ASCE, 1998) was the necessity for further basic research on bank erosion and channel narrowing. Significant efforts have been devoted in the last few years to investigate for instance, the effects of removing a dam on the transient response and final equilibrium achieved by the affected river. Morphological evaluations have been restricted however, to field monitoring of that response and to qualitatively describing some of the processes involved (Doyle et al., 2003).

Experiments on sedimentation and erosion processes in reservoirs performed at St. Anthony Falls Laboratory (Cantelli et al., in press) have shown an interesting phenomenon herein called "erosional narrowing". This occurs immediately after the sudden ("blow and go") removal of a dam that is filled with sediment. A channel incises into the deposit after failure of the leading front of the deposit. In the early stages of incision this channel may become significantly narrower as it undergoes degradation, in particular within the reach immediately upstream of the original location of the dam. Channel incision and narrowing propagate in the upstream direction for a very short time compared to the final channel widening adjustment towards a new equilibrium state (see Figure 1). This observation is contrary to the general belief that the incisional channel widens from the very beginning (Schumm et al., 1994), hence its inclusion should lead to an improved understanding and prediction capability of morphological evolution for spatial and temporal scales larger than the ones related to erosional narrowing only.

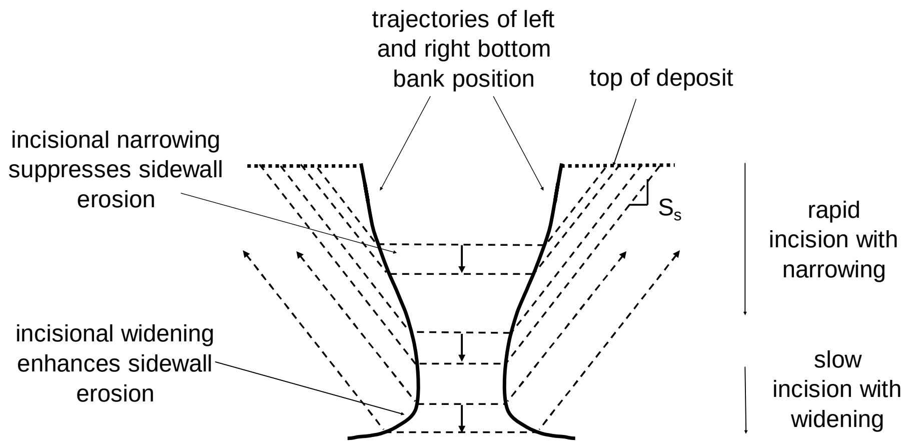

Figure 1. Sketch of the process of incision into a reservoir deposit.

Erosional narrowing is hypothesized to occur as a result of the lateral variation of the boundary shear stress, from a higher value at the channel center to a lower value along the bank regions. Under conditions of sufficiently rapid degradation, the contribution of sediment from the sidewalls cannot keep up with bed degradation, and as a result the channel narrows. As the degradation rate drops narrowing gives way to widening.

Theoretical formulation

Model definition and assumptions

A 1-D model approximation is used to simulate the phenomenon of erosional narrowing observed in the experiments carried out by Cantelli et al. (in press). This model derives from the “Sediment Digester” (Parker, 2004), a model which was designed to track the channel bed elevation and bottom width of a river when subjected to input of sediment from one of its banks from a mine-derived earthflow. While the original model was designed for an aggradational setting, it is here adapted to a degradational setting. Figure 2 shows a sketch of the conceptual model of the counteracting effects of the two main processes explaining the time evolution of erosional narrowing, i.e. the streamwise sediment transport imbalance due to incision and the depositional contribution from the channel bank erosion.

The definitions used in Figure 2 are: x = streamwise coordinate (directed into the page), y = transverse coordinate (origin at the center of the channel and positive toward the right bank), S_s = slope of the channel banks (constant value), H = water depth (defining the active channel), B_b = half the channel width on the bed region, B_w = half the top width on the active channel, B_s = width of one sidewall region (including both submerged and emergent banks), η_b = bed elevation on the bed region, η_t = elevation of the top of the active channel, and η_e = elevation of the top of the channel bank. The following geometrical relationships can be established, with the sub-indices denoting the locations/dimensions indicated in Figure 2:

$$y_b = B_b; \qquad y_e = B_b + B_s \qquad (1a; 1b)$$

$$H = \eta_t - \eta_b \qquad (1c)$$

$$B_s = \frac{\eta_e - \eta_b}{S_s}; \qquad B_w = B_b + \frac{H}{S_s} \qquad (1d; 1e)$$

The simplifications used in the formulation of the 1-D model are the assumption of a straight channel with trapezoidal cross-section of constant sidewall slope, the normal flow approximation (uniform and steady), non-cohesive and uniform bed sediment, and fluvial transport of sediment as bedload only.

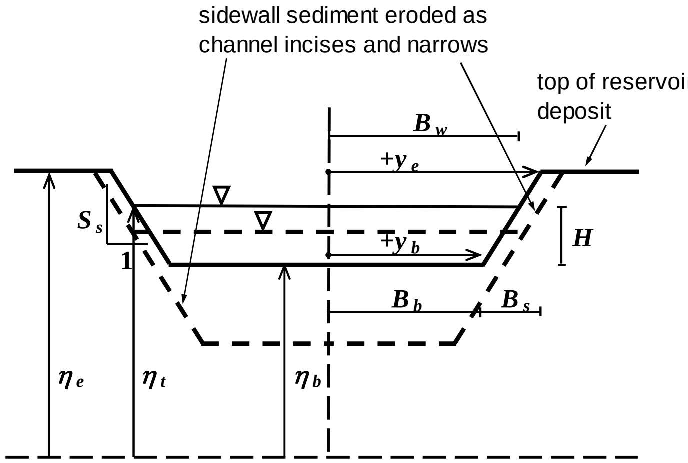

Figure 2. Sketch of the conceptual model for erosional narrowing. Cross-section at time t: solid line; cross-section at time $t+\Delta t$: dashed line.

<u>Channel hydraulics and sediment transport rates</u>

The combination of the equation for conservation of streamwise momentum under steady and uniform flow conditions, the Manning-Strickler flow resistance relation and the water continuity equation allows one to compute the water depth, H, when sidewall effects are negligible:

$$H = \left(\frac{k_s^{1/3} Q_w^2}{4\alpha_r^2 g B_b^2 S_0} \right)^{3/10}; \qquad S_0 = -\frac{\partial \eta_b}{\partial x} \qquad (2a; 2b)$$

where k_s = bed roughness height ($k_s \approx n_k D_{90}$, $n_k \sim 2\text{-}4$), D_{90} = grain size for which 90% of the material in the bed surface is finer, Q_w = water discharge, $\alpha_r \approx 8.10$, g = gravitational acceleration, and S_0 = bed slope in the streamwise direction. It can be shown that for a hydraulically wide channel (aspect ratio $H/B_b \leq 0.10$) and sediment Coulomb friction angles in the range $25° \leq \phi \leq 40°$, sidewall effects are indeed not important.

The dimensionless boundary shear stresses (Shields numbers) for the bed and the sidewall regions (τ_b^* and τ_s^*, respectively) can be computed from:

$$\tau_b^* = \frac{\tau_{bb}}{\rho R g D} = \frac{H S_0}{R D}; \qquad \tau_s^* = \varphi \tau_b^* \qquad (3a; 3b)$$

where ρ = density of water, R = submerged specific gravity of the sediment ($R = \rho_s/\rho - 1$), ρ_s = density of the sediment, D = median grain size diameter of the sediment in the bed surface, and φ = number relating the boundary shear stress on the sidewall region of the active channel, τ_{bs}, to the one on the bed region, τ_{bb}, which typically varies between 0.40 and 0.80 ($\tau_{bs} = \varphi\tau_{bb}$). From equations (2) and (3a), it becomes evident that the boundary shear stress is a function of B_b and S_0:

$$\tau_b^* = \frac{1}{RD}\left(\frac{k_s^{1/3} Q_w^2}{4\alpha_r^2 g}\right)^{3/10} B_b^{-3/5} S_0^{7/10} \tag{4}$$

The streamwise volume bedload transport rate per unit width on the bed and the sidewall regions (q_{bsb} and q_{bss}, respectively) is then computed from a common bedload transport relation using the appropriate shear stress values. Here Parker's approximation of the Einstein bedload transport relation (Parker, 1979) is used:

$$q_{bsb} = \sqrt{RgD}D\alpha_s\left(\tau_b^*\right)^{1.5}\left(1 - \frac{\tau_c^*}{\tau_b^*}\right)^{4.5} \tag{5a}$$

$$N_{qr} = \frac{1}{\varphi^3}\left(\frac{\varphi\tau_b^* - \tau_c^*}{\tau_b^* - \tau_c^*}\right)^{9/2}; \qquad q_{bss} = N_{qr} q_{bsb} \tag{5b; 5c}$$

where $\alpha_s \approx 11.20$, τ_c^* = Shields number for incipient particle motion ($\tau_c^* \approx 0.030$), and N_{qr} is a dimensionless number. Let q_{bs} denote the total volume bedload transport rate per unit width in the streamwise direction, and q_{bn} denote the corresponding one in the transverse (normal) flow direction. According to Parker and Andrews (1985):

$$\frac{q_{bn}}{q_{bs}} = \frac{\tau_{bn}}{\tau_s} - \alpha_n\sqrt{\frac{\tau_c^*}{\tau_s^*}}\frac{\partial\eta}{\partial y} \tag{6}$$

where τ_{bn} = boundary shear stress in the transverse direction, τ_s = boundary shear stress in the streamwise direction ($\tau_s = \tau_{bs}$ for the sidewall region), and $\alpha_n \approx 2.65$ (after Johannesson and Parker, 1989). For secondary flows assumed negligible, τ_{bn} can be approximated as vanishing. Moreover, if the bed region is considered horizontal ($\partial\eta/\partial y = 0$), q_{bn} = zero. In the sidewall region however, where $q_{bs} = q_{bss}$ and $\partial\eta/\partial y = S_s$, the volume bedload transport rate per unit width at the sidewall region in the transverse direction, q_{bns}, may be estimated from:

$$q_{bns} = -q_{bss}\alpha_n\sqrt{\frac{\tau_c^*}{\varphi\tau_b^*}}S_s \qquad \hat{q}_{bns} = -q_{bns} \tag{7a; 7b}$$

It is seen from equations (2a) to (7b) that as the channel bottom width gets narrower, both the water depth and the Shields numbers increase, which in turn implies that the sediment transport increases and therefore, the river's capacity to erode the channel banks is increased as well.

Sediment continuity in the bed and sidewall regions

The Exner sediment continuity equation in two dimensions can be written as:

$$\left(1 - \lambda_p\right)\frac{\partial\eta}{\partial t} = -\frac{\partial q_{bs}}{\partial x} - \frac{\partial q_{bn}}{\partial y} \tag{8}$$

where t = time, and λ_p = porosity of the sediment on the bed deposit (constant value). Equation (8) can be integrated over half the bed region (from 0 to $+y_b$), and reduced with Leibnitz' rule to obtain:

$$\left(1-\lambda_p\right)\frac{\partial \eta_b}{\partial t} = -\frac{\partial q_{bsb}}{\partial x} + \frac{\hat{q}_{bns}}{B_b} \qquad (9)$$

where $\hat{q}_{bns}$ is obtained from equation (7b), and is a positive quantity representing the value of q_{bn} evaluated at $+y_b$. Thus, the second term on the right-hand side of equation (9) accounts for the sediment contribution towards aggradation in the bed region as a result of the fluvial erosion of the channel banks/sidewalls. The incisional character of the sediment transport imbalance in the streamwise direction, i.e. the first term on the right-hand side of equation (9), creates a counteracting effect. As such, when sidewall erosion accompanies degradation, the sidewall erosion suppresses (but does not stop) degradation.

Equation (8) can also be integrated over the whole sidewall region (from $+y_b$ to $+y_e$), i.e., including both the submerged and emergent regions. Again applying Leibnitz' rule, the fact that no sediment transport occurs above the water surface elevation, using and equations (1a), (1b) and (1e), and assuming that $q_{bs} = q_{bss}$ on the sidewall region, equation (8) may be reduced to:

$$\left(1-\lambda_p\right)B_s\left(\frac{\partial \eta_b}{\partial t} - S_s\frac{\partial B_b}{\partial t}\right) = -\frac{\partial}{\partial x}\left(q_{bss}\frac{H}{S_s}\right) - q_{bss}\frac{\partial B_b}{\partial x} - \hat{q}_{bns} \qquad (10)$$

The combination of equations (9) and (10) gives rise to the governing equation for the time evolution of the channel width as follows:

$$\left(1-\lambda_p\right)\frac{\partial B_b}{\partial t} = -\frac{1}{S_s}\frac{\partial q_{bsb}}{\partial x} + \frac{1}{S_s}\frac{\left(B_s+B_b\right)}{B_sB_b}\hat{q}_{bns} + \frac{1}{S_s}\left[\frac{q_{bss}}{B_s}\frac{\partial B_w}{\partial x} + \frac{H}{B_sS_s}\frac{\partial q_{bss}}{\partial x}\right] \qquad (11)$$

Immediately after the removal of a dam, an incisional channel can be expected to form and degrade rapidly, in which case $\partial q_{bsb}/\partial x > 0$. This in turn drives a strongly downward-concave long profile. Thus the first term on the right-hand side of equation (11) is always negative, leading to a reduction of the channel width. This is the dominant process during erosional narrowing. Contrarily, the second term on the right-hand side of equation (11), i.e. the one accounting for sediment contribution from the channel banks/sidewalls as a result of fluvial erosion, is always positive, hence favoring channel widening. The last term on equation (11) may be either positive or negative, but dimensional analysis indicates it is usually an order of magnitude smaller than the other two.

Summarizing, equations (9) and (11) constitute the 1-D formulation for the time evolution of the channel bed elevation and bottom width, η_b and B_b respectively, of a river reach going through erosional narrowing (as well as subsequent widening).. Based on the experiments performed by Cantelli et al. (in press), we assume that the reach upstream of the original dam degrades around a 'pivot' point located immediately upstream of the removed dam. The model does not yet explicitly include the aggradational region located downstream of the removed dam.

Partial derivatives and dimensionless numbers

The different partial derivative terms in equations (9) and (11) can be reduced to functions of the channel bottom width, B_b, and bed slope, S_0. For instance, by defining the following dimensionless numbers:

$$N_{qb} = \frac{\tau_b^*}{q_{bsb}} \frac{\partial q_{bsb}}{\partial \tau_b^*} = \frac{3}{2} + \frac{9}{2} \frac{\tau_c^*}{\left(\tau_b^* - \tau_c^*\right)} \tag{12a}$$

$$N_{\tau S_0} = \frac{S_0}{\tau_b^*} \frac{\partial \tau_b^*}{\partial S_0} = \frac{7}{10}; \qquad N_{\tau B} = -\frac{B_b}{\tau_b^*} \frac{\partial \tau_b^*}{\partial B_b} = \frac{3}{5} \tag{12b; 12c}$$

and using equations (5a) and (4), the streamwise gradient of the sediment transport becomes:

$$\frac{\partial q_{bsb}}{\partial x} = N_{qb} \left(N_{\tau S_0} \frac{q_{bsb}}{S_0} \frac{\partial S_0}{\partial x} - N_{\tau B} \frac{q_{bsb}}{B_b} \frac{\partial B_b}{\partial x} \right) \tag{13a}$$

Equation (9) then becomes:

$$\left(1 - \lambda_p\right) \frac{\partial \eta_b}{\partial t} = -N_{qb} \left(N_{\tau S_0} \frac{q_{bsb}}{S_0} \frac{\partial S_0}{\partial x} - N_{\tau B} \frac{q_{bsb}}{B_b} \frac{\partial B_b}{\partial x} \right) + \frac{\hat{q}_{bns}}{B_b} \tag{13b}$$

Accordingly, by defining additional dimensionless numbers of the form:

$$N_{qs} = \frac{\tau_b^*}{q_{bss}} \frac{\partial q_{bss}}{\partial \tau_b^*} = \frac{3}{2} + \frac{9}{2} \frac{\tau_c^*}{\left(\varphi \tau_b^* - \tau_c^*\right)} \tag{14a}$$

$$N_{HS_0} = -\frac{S_0}{H} \frac{\partial H}{\partial S_0} = \frac{3}{10}; \qquad N_{HB} = -\frac{B_b}{H} \frac{\partial H}{\partial B_b} = \frac{3}{5} \tag{14b; 14c}$$

which can be collapsed together with equations (5b) and (12a)-(12c) into:

$$N_{S_0} = N_{qb} N_{\tau S_0} - \frac{H}{S_s B_s} N_{qr} \left(N_{qs} N_{\tau S_0} - N_{HS_0} \right) \tag{15a}$$

$$N_B = N_{qb} N_{\tau B} + N_{qr} \left[\frac{B_b}{S_s} - \frac{H}{S_s B_s} \left(N_{qs} N_{\tau B} + N_{HB} \right) \right] \tag{15b}$$

the governing equation for the time evolution of the channel bottom width becomes:

$$\left(1 - \lambda_p\right) S_s \frac{\partial B_b}{\partial t} = -N_{S_0} \frac{q_{bsb}}{S_0} \frac{\partial S_0}{\partial x} + N_B \frac{q_{bsb}}{B_b} \frac{\partial B_b}{\partial x} + \hat{q}_{bns} \frac{\left(B_b + B_s\right)}{B_b B_s} \tag{16}$$

It is easy to realize, in a similar fashion to the physical interpretation of equation (11), that the first term on the right hand-side of equation (16) is negative for a bed slope increasing in the downstream direction (concave-downward long profile), hence forcing channel narrowing. On the other hand, the last term in equation (16) is always positive, therefore contributing to channel widening.

Critical condition for inception of erosional narrowing

One interesting observation from the experiments by Cantelli et al. (in press) is that erosional narrowing does not always occur after the sudden removal of a dam. Therefore, a critical condition for inception of this phenomenon should exist. A first attempt at defining this condition follows.

The channel width decreases in time during erosional narrowing; that is, $\partial B_b/\partial t \leq 0$. If the channel reach where erosional narrowing is concentrated corresponds to a section of approximately constant width in the longitudinal direction, the partial derivative in space of B_b vanishes ($\partial B_b/\partial x = 0$). In consequence, equation (16) can be re-arranged to determine the downward concavity in the streamwise bed profile required for erosional narrowing to occur. This downward concavity is expressed in terms of the condition $\partial S_0/\partial x > 0$. The required degree of downward concavity is expressed in dimensionless form in equation (17a):

$$\frac{B_b}{S_0}\frac{\partial S_0}{\partial x} \geq M\,\frac{\left(B_b + B_s\right)}{B_b B_s}\sqrt{\frac{\tau_c^*}{\tau_b^*}}S_s \qquad M = \frac{N_{qr}}{N_{S_0}}\frac{\alpha_n}{\sqrt{\varphi}} \qquad \text{(17a; 17b)}$$

Numerical implementation

Initial and boundary conditions

The transformed equations (13b) and (16) represent the governing equations for the time evolution of the bed elevation in the bed region η_b, and the channel bottom width B_b, respectively. Since both these coupled partial differential equations are highly non-linear, they are solved numerically. One initial condition and two boundary conditions are required for η_b in equation (13b), while one initial condition and only one boundary condition are needed for B_b in equation (16).

The initial condition for η_b corresponds to the final longitudinal profile of the progradational delta front resulting from the previous dam-induced sedimentation. On the other hand, the initial conditions for B_b are set in such a way that streamwise sediment transport occurs in the bed region but not on the channel banks of a reach well upstream of the dam. This reach has the lowest streamwise bed slope (see Figure 3). From equations (5b) and (5c), the criterion of vanishing sediment transport in the sidewall regions translates into:

$$\tau_b^* = \frac{\tau_c^*}{\varphi} \qquad (18)$$

Recalling the definition of the boundary shear stress of equation (4), B_b at time $t = 0$ can be computed from:

$$B_b = \left[\frac{1}{RD}\left(\frac{k_s^{1/3} Q_w^2}{4\alpha_r^2 g}\right)^{3/10}\frac{\varphi}{\tau_c^*}\right]^{5/3}\left(S_0\big|_{u/s}\right)^{7/6} \qquad (19)$$

where the subscript u/s on S_0 above denotes the upstream end of the reach. The computed value for B_b at $t = 0$ is also used for the whole length of the channel, including the steeper sector at the downstream end, as a convenient initial condition.

The first boundary condition for η_b is derived from actual measurements by Cantelli et al. (in press). These experiments show a 'pivot' point immediately upstream of the original location of the dam removed, for which the bed elevation remains approximately constant (see Figure 3):

$$\eta_b\big|_{d/s} = 0 \qquad (20)$$

where the subscript d/s denotes downstream end of the channel reach.

The second boundary condition for η_b is derived from the assumption of a constant total volume sediment supply at the upstream end of the channel, $Q_{bs}|_f$. The latter may be computed from the general expression for the total volume sediment transport rate, Q_{bs}:

$$Q_{bs} = B_b q_{bsb} + \frac{H}{S_s} q_{bss} \tag{21}$$

By using the initial conditions of equations (18) and (19), and the definition of q_{bsb} given in equation (5a), it is found that $Q_{bs}|_f$ can be computed as:

$$Q_{bs}\Big|_f = \frac{\alpha_s k_s^{1/6} Q_w}{2\alpha_r R^{7/6} D^{1/6}} \frac{\varphi^{1/6}(1-\varphi)^{4.5}}{\left(\tau_c^*\right)^{1/6}} \left(S_0\big|_{u/s} \right)^{7/6} \tag{22}$$

Thus, a boundary condition at the upstream end is specified in terms of upstream bed slope as a function of flow discharge and upstream sediment feed rate.

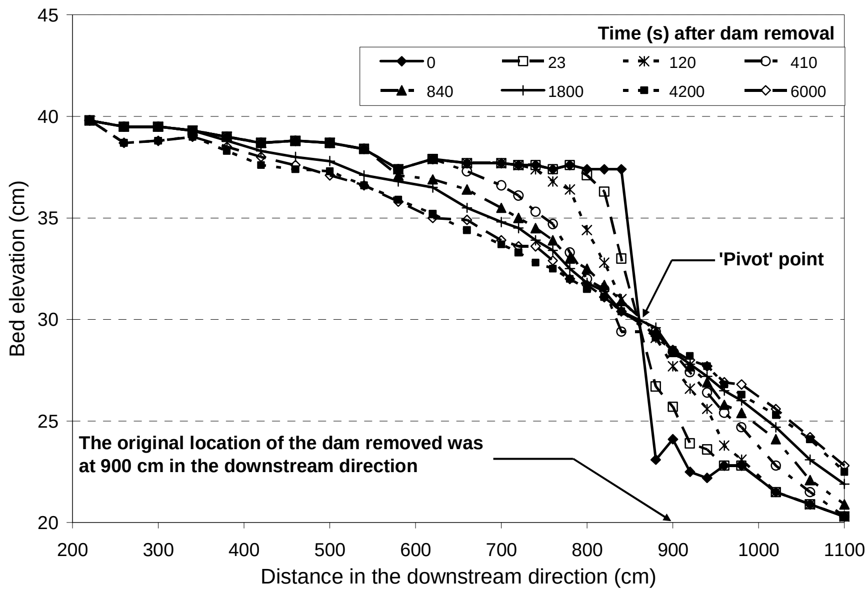

Figure 3. Long profile measured in Experiment # 5 by Cantelli et al. (in press).

The transformed partial differential equation (16) is a wave-type equation of first order in time, which can be re-arranged in the following form:

$$\frac{\partial B_b}{\partial t} - N_B \frac{1}{\left(1-\lambda_p\right)S_s} \frac{q_{bsb}}{B_b} \frac{\partial B_b}{\partial x} = \frac{-N_{S_0} \frac{q_{bsb}}{S_0} \frac{\partial S_0}{\partial x} + \hat{q}_{bns} \frac{\left(B_b + B_s\right)}{B_b B_s}}{\left(1-\lambda_p\right)S_s} \tag{23}$$

As mentioned above, dimensional analysis shows that the term in between brackets in equation (15b) is an order of magnitude smaller than the other one the right-hand side. Because both dimensionless numbers N_{qb} and $N_{\tau B}$ are positive in that relation, N_B must be positive, and hence the sign of the advective term in equation (23) is negative. This further implies wave-like behavior propagating from downstream to upstream, so that the boundary condition for B_b must be specified at the downstream end of the channel. A reasonable assumption is that the 'pivot' point above referred also constitutes an inflection point in the sediment load, so that:

$$\left.\frac{\partial Q_{bs}}{\partial x}\right|_{d/s} = 0 \tag{24}$$

Beginning with the general expression for Q_{bs} given in equation (21), partial derivatives with respect to x are computed using the dimensionless numbers defined in equations (5b), (12a)-(12c) and (14a)-(14c). After some algebra and the dropping of several terms that can be demonstrated to be small, it is found that the following mixed (Robin) boundary condition for B_b holds at the downstream end of the channel:

$$\frac{\partial B_b}{\partial x} - \frac{\frac{\partial S_0}{\partial x}}{S_0}\frac{N_{qb}N_{\tau S_0}}{\left(N_{qb}N_{\tau B} - 1\right)}B_b = 0 \tag{25}$$

<u>Sample numerical run</u>

A sample and preliminary numerical calculation was performed using Experiment # 5 of Cantelli et al. (in press). The following parameters were used: reach length L = 6.4 m, n_k = 4.0, α_r = 8.1, α_s = 11.2, τ_c^* = 0.024, α_n = 2.65, φ = 0.50, R = 1.67, D = 0.80 mm, Q_w = 0.3 L/s, λ_p = 0.40, and S_s = 0.41 (22.5°). In addition, D_{90} was estimated from D and the geometric standard deviation of the sediment mixture σ_g of 1.71.

Figure 4 shows a comparison of calculated and measured long profiles of water surface at time t = 1200 sec. Figure 5 shows a comparison of the time evolution of observed and predicted channel water surface width at a point located 0.90 m upstream of the original position of the dam. While the agreement is not perfect, the model clearly captures a) the strongly downward-concave long profile evolving after dam removal, and more importantly b) rapid erosional narrowing followed by slow erosional widening.

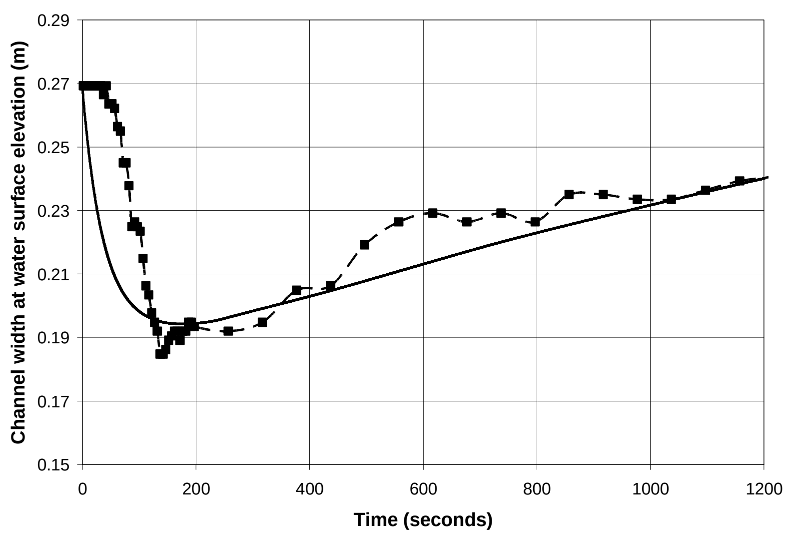

Figure 4. Calculated (solid line) and measured (dashed line with filled squares) time evolution of channel surface width at a point 0.9 m upstream of the original dam position.

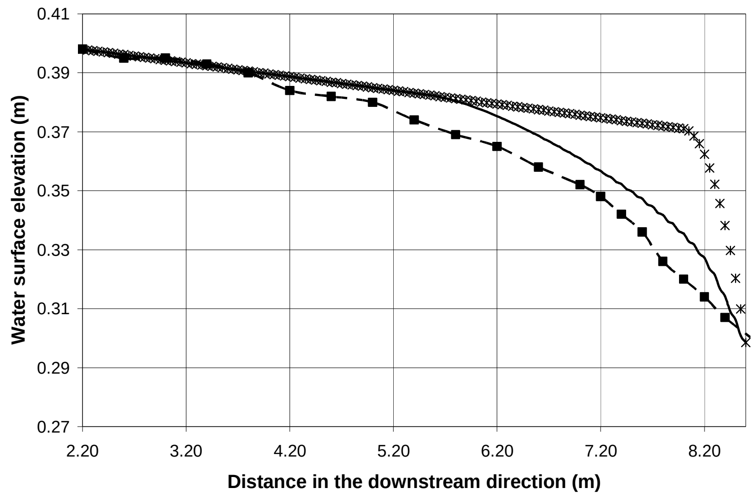

Figure 5. Assumed initial water surface long profile right after dam removal (crosses), and calculated (solid line) and measured (dashed line with filled squares) water surface long profiles 1200 sec after removal.

Conclusions

The theoretical development presented here explains erosional narrowing in terms of a competition between rapid bed degradation, which enhances narrowing, and input of eroded sediment from the sidewalls, which suppresses it. A first numerical implementation proves capable of capturing the essential aspects of the phenomenon.

This material is based upon work funded by the National Science Foundation under agreement number EAR-0207274, as well as the STC Program under agreement number EAR-0120914.

References

ASCE Task Committee on Hydraulics, Bank Mechanics and Modeling of River Width Adjustment (1998). "River Width Adjustment. II: Modeling." *Journal of Hydraulic Engineering*, ASCE, 124(9), 881-902.

Cantelli, A., Paola, C., and Parker, G. (in press). "Experiments on upstream-migrating bed and bank erosion induced by dam removal." *Water Resources Research*.

Doyle, M. W., Stanley, E. H., and Harbor, J. M. (2003). "Channel adjustments following two dam removals in Wisconsin." *Water Resources Research*, 1, 1011, doi:10.1029/2002WR001714.

Johannesson, H., and Parker, G. (1989). "Linear Theory of River Meanders." *River Meandering*, S. Ikeda and G. Parker, eds., Water Resources Monograph 12, American Geophysical Union, Washington, D.C., 181-214.

Parker, G. (1979). "Hydraulic Geometry of Active Gravel Rivers." *Journal of the Hydraulics Division*, ASCE, 105(HY9), 1185-1201.

Parker, G., and Andrews, E. D. (1985). "Sorting of Bed Load Sediment by Flow in Meander Bends." *Water Resources Research*, 21(9), 1361-1373.

Parker, G. (2004). "The Sediment Digester." *Internal Memorandum*, St. Anthony Falls Laboratory, University of Minnesota, Minneapolis, Minnesota.

Schumm, S. A., Harvey, M. D., and Watson, C. C. (1984). *Incised channels: Morphology, dynamics and control*. Water Resources Publications, Littleton, Colorado.